Solid Inclusion Complexes of α-Cyclodextrin and Perdeuterated Poly(oxyethylene)

Tom E. Girardeau, Tiejun Zhao, Johannes Leisen, and Haskell W. Beckham*

School of Polymer, Textile and Fiber Engineering, Georgia Institute of Technology, Atlanta, Georgia 30332-0295

David G. Bucknall†

Department of Materials, Oxford University, Oxford, Parks Road, Oxford, OX1 3PH, U.K.

Received June 22, 2004; Revised Manuscript Received December 21, 2004

ABSTRACT: Solid inclusion complexes were prepared by solution precipitation of α-cyclodextrin (α-CD) and monodisperse poly(oxyethylene)s (POEs). The POE was either perdeuterated with molecular weights from 1.5 to 59.2 kg/mol or fully hydrogenated with molecular weights from 1.5 to 86.6 kg/mol. The number of cyclodextrins per chain increased linearly with molecular weight for both backbones. For a given chain length (X_n), the perdeuterated POE backbone precipitated with a larger number of cyclodextrins than the hydrogenated POE. Assuming all of the cyclodextrins are threaded, the fractional coverage of the backbones decreases with increasing POE chain length but plateaus for chain lengths just below $X_n \approx 500$. At this chain length, the threading time becomes significantly longer (400 min) for perdeuterated POE as compared to the hydrogenated POE (28 min). Under the standard aqueous precipitation procedure, solid inclusion complexes could not be formed using perdeuterated POE with chain lengths greater than 1230 repeat units (59.2 kg/mol). Morphologies of the solid complexes were examined with wide-angle X-ray diffraction (WAXD) and small-angle neutron scattering (SANS). For molecular weights >3.2 kg/mol, POE backbones are partially covered with cyclodextrins that aggregate to form crystalline hydrogen-bonded stacks of α-CD-threaded POE separated by amorphous layers of unthreaded POE. As the POE molecular weight increases, the size of the crystalline α-CD stacks decreases. For molecular weights of 44 kg/mol ($X_n = 917$), the stack size has decreased to the point that the materials exhibit very low crystallinity, even though 83% of the chain is covered with cyclodextrins. This low crystallinity is in contrast to the complex prepared from a hydrogenated chain of similar molecular weight (48.5 kg/mol), which exhibits higher crystallinity but is threaded by fewer cyclodextrins. These distinctive morphologies are related to the formation kinetics for these α-cyclodextrin inclusion complexes.

Introduction

Spontaneous threading of cyclodextrins onto linear polymers, followed by precipitation or gelation, occurs in solution when both species are present above a critical concentration. Harada et al. reported the first example of such cyclodextrin-rotaxanated polymers formed via self-assembly using poly(ethylene glycol) and α-cyclodextrin.[1] These solid-state inclusion complexes do not form when there are less than four oxyethylene repeat units in the glycol.[2] For longer backbones up to about 30 oxyethylene units, full coverage occurs before precipitation of the complex; the ratio of polymer repeat units (PRU) to cyclodextrin (CD) in these crystalline inclusion complexes is at least 2:1.[3] This ratio increases (signifying decreased threading) for chain lengths beyond about 30 oxyethylene units because gelation occurs and prevents continued threading.[4] Gel formation occurs when some minimum number of cyclodextrins have threaded, form hydrogen-bonded stacks,[5] and aggregate with stacks on other segments to yield physical cross-links. These cross-links may be reversibly dissociated by heating or solvation. This phenomenon has been exploited to create a thermoreversible hydrogel by grafting poly(ethylene glycol) (PEG) segments onto polymers such as dextran.[6] These supramolecular hydrogels have been proposed for use in drug delivery applications.[7]

The rate of precipitation or gelation of the polymer−cyclodextrin complex can be followed with turbidity measurements. Harada showed the rate reached a maximum for a PEG with 22 oxyethylene repeat units (1000 g/mol) and suggested the rate decrease with higher molecular weights was due partly to the decreasing concentration of end groups.[1] For a given molecular weight, the threading rate can be slowed by adding bulky[8] or positively charged[9] groups onto the chain ends. Ceccato et al. studied PEG with an average of 75 oxyethylene units and referred to the time to gel as the threading time, t_{th}.[10] At room temperature in water, t_{th} is about 200 s; this value decreases when water is replaced with heavy water and increases when urea is added to the solution. For all solutions, t_{th} increased with increasing temperature, reaching nearly 1000 s for water at 40 °C. These observations are consistent with a complexation rate that decreases (t_{th} increases) as the hydrogen-bonding capacity of the medium increases. Using a transition-state model, they calculated 20 ± 2 α-CD macrocycles threaded per chain for an average PRU:CD ratio of 3.8, slightly higher than the PRU:CD ratio of 3 that is found experimentally.[11]

The same experimental approach and model were also applied to the threading of β-cyclodextrin onto poly(propylene glycol).[12] As with the α-CD/PEG material, threading was retarded by the addition of urea or increasing the temperature. An alternative means for

* Author to whom correspondence should be addressed. E-mail: haskell.beckham@ptfe.gatech.edu.

† Present address: School of Polymer, Textile and Fiber Engineering, Georgia Institute of Technology, Atlanta, GA 30332-0295.

10.1021/ma048756w CCC: $30.25
Published on Web 02/10/2005

controlling the threading kinetics is the addition of ions, which were found to increase or decrease the threading time depending on their polarizability.[13] This effect was opposite for anions and cations. For example, while fluoride caused an increase in t_{th}, the more polarizable iodide caused a decrease; Li^+ decreased t_{th} while the more polarizable Cs^+ increased t_{th}. Interestingly, 0.1 M sodium hydroxide had minimal influence on t_{th} (~8% increase), despite the accompanying pH change.[14] In fact, all ions caused relatively minor changes in the threading times compared to those caused by adding urea or increasing temperature.

If the goal is threading as many cyclodextrins as possible onto polymer backbones, then t_{th} should be increased by postponing gelation. One of the most effective means for doing this is apparently increasing the temperature of the originating solutions. This strategy has been employed for the preparation of inclusion complexes from a variety of linear polymers.[15−21] If the goal is a thermoreversible gel with supramolecular physical cross-links, a number of experimental variables are available for controlling t_{th}[10,12−14] and, thus, the size of the threaded segments. The size of the threaded segments should influence the size of the physical cross-links which govern the thermal and mechanical stability of the gel. However, quantitative relationships between threading time, threaded segment length, and physical properties of the thermoreversible gels have not yet been reported.

We report here some relationships between the synthesis and morphology of cyclodextrin-rotaxanated polymers. Monodisperse poly(oxyethylene) (POE) and monodisperse perdeuterated POE were threaded with α-cyclodextrin. Threading times, ratios, and yields are reported as a function of backbone molecular weight. The resulting inclusion complexes were examined with solid-state ^{13}C NMR spectroscopy, wide-angle X-ray diffraction (WAXD), and small-angle neutron scattering (SANS). The goal of these studies is to define some synthesis/structure/property relationships in rotaxanated polymers.

Experimental Details

Materials. Chemicals were purchased from commercial suppliers and used as received. Pharmaceutical-grade α-CD was obtained from Wacker Biochem. Unless indicated otherwise, POEs were obtained from Polymer Source. The POE samples were α-hydroxy-ω-ethyl terminated, with the exception of the 1.5- and 3.4-kg/mol hydrogenated samples, which were α,ω-dihydroxy terminated. All polymers were characterized by polydispersities between 1.04 and 1.1. Specific POEs are referred to in this paper using the polymer abbreviation with a subscript for the number-average degree of polymerization (X_n). For example, *d*-POE_{31} is the perdeuterated poly(oxyethylene) with $X_n = 31$.

Rotaxanated Polymer Formation. Unless otherwise indicated, POE/CD inclusion complexes were prepared by combining an aqueous solution of POE (150 mg POE in 3 mL of H_2O) with an aqueous solution of α-CD (1.45 g CD in 8 mL of H_2O) in a 20-mL vial. The ratio of PRU to α-CD in this originating solution is 2.3. The initially clear solution was ultrasonically agitated for 10 min and then kept at room temperature for about 16 h. A white gel formed during this time. The gel was placed in a beaker containing an additional 11 mL of distilled H_2O, swirled for 10−15 s to dissolve unthreaded components, and collected via filtration in a Buchner funnel. The products were then dried overnight under vacuum at 50 °C to give white powders. Yields, reported in Tables 1 and 2, refer to the weight of the dry product complex compared to the total weight of the starting materials.

Table 1. α-Hydroxy-ω-ethyl Poly(oxyethylene)s[a] and Their α-Cyclodextrin Complexes

POE		POE-*pseudorotaxa*-αCD				
M_n (kg/mol)	X_n	yield (%)	PRU:CD[b]	CD/chain	% maximum coverage[c]	t_{th} (min)
1.5[a,d]	34	66	2.7	13	88	0.26
3.4[a]	77	69	3.0	26	78	0.67
14.3	325	66	3.5	93	66	5.7
22.3	507	66	3.6	140	64	10
48.5	1100	57	3.7	300	63	28
86.6	1970	64	3.6	550	64	33

[a] M_n = 1.5 and 3.4 kg/mol are α,ω-dihydroxy terminated. [b] Polymer repeat units per cyclodextrin, determined by ^1H NMR. [c] Assuming all CDs are threaded, =100[(PRU:CD in originating solution)/(PRU:CD)]. [d] Polysciences.

Table 2. Perdeuterated α-Hydroxy-ω-ethyl Poly(oxyethylene)s and Their α-Cyclodextrin Complexes

d-POE		*d*-POE-*pseudorotaxa*-αCD				
M_n (kg/mol)	X_n	yield (%)	PRU:CD[a]	CD/chain	% maximum coverage[b]	t_{th} (min)
1.5[c]	31	61	2.7	12	100[d]	0.33
3.2	67	66	2.5	27	93	0.5
16.5	344	70	2.6	130	87	4.5
25.8	538	54	2.7	200	86	22
44	917	36	2.8	330	83	400
59.2	1230	6.3	3.5	350	65	–

[a] Polymer repeat units per cyclodextrin, determined by ^{13}C NMR. [b] Assuming all CDs are threaded, =100[(PRU:CD in originating solution)/(PRU:CD)]. [c] Cambridge Isotopes. [d] PRU:CD = 2.7 in the originating solution for 1.5-kg/mol *d*-POE; 2.3 for all other samples.

A physical blend was prepared by dissolving POE and α-CD in DMSO, a solvent in which POE and α-CD exist as unthreaded components,[8] followed by vacuum-drying. This blend was then washed with water according to the same procedure described above; no solid remained, suggesting this washing procedure was effective at removing unthreaded components.

Nuclear Magnetic Resonance. Threading levels are reported as the number of PRU per CD. PRU:CD ratios were determined from NMR spectra of the inclusion complexes dissolved in DMSO-d_6. In this solvent, these polypseudorotaxanes dethread rapidly and exist as two separate components.[8] For the hydrogenated POE complexes, ^1H NMR spectroscopy was employed to determine the relative peak area of the CD methine proton at 4.79 ppm to that of POE at 3.5 ppm. ^1H NMR spectra were collected on a Bruker DRX 500 spectrometer. Single-pulse excitation was employed using a 30° pulse length and 5-s recycle delay; 16 scans were collected. For the perdeuterated POE complexes, ^{13}C NMR spectroscopy was employed. ^{13}C NMR spectra were collected on a Bruker AMX 400 spectrometer using an inverse-gated decoupling sequence, 90° pulse lengths, and 60-s recycle delays; 5120 scans were collected. For more rapid acquisitions, chromium (III) acetylacetonate was added as a relaxation agent and a 1-s recycle delay was employed. Relative peak intensities were equivalent to the spectra collected with a 60-s recycle delay, thus verifying that the 1-s recycle delay was sufficiently long when using the relaxation agent.

The PRU:CD ratios are shown in Tables 1 and 2. Increasing PRU:CD ratios signify decreased threading levels. Given the dimensions of the POE monomer and α-CD, a PRU:CD ratio of 2 represents the maximum threading level. The values shown in Tables 1 and 2 were determined after washing the complexes with a single 11-mL dose of water as described in the preceding section. To examine the effect of washing on the PRU:CD ratio, an inclusion complex was formed with a 20-kg/mol POE and washed four times (a wash is defined as swirling 10−15 s in 11 mL of water). The sample weight and PRU:CD ratio were determined after each of the four washes and found to be equivalent.

Solid-state ^{13}C NMR spectroscopy was conducted on a Bruker DSX 300. A cross-polarization pulse sequence was employed with a 2.5-ms contact time and a 4-s recycle delay. Spectra were collected while magic-angle spinning at 5 kHz. The number of scans was 1.5k, the spectral width was 25 kHz, and 2k complex data points were acquired.

Solution Turbidity. UV/vis spectra of the POE/CD originating solutions were collected on a Shimadzu UV16OU UV/visible recording spectrometer at 700 nm and 21 °C with H_2O in the reference cell. The onset of solution turbidity was defined as the time when the absorbance reached 0.05. The experiments were conducted by combining the POE and CD solutions in the sample cell in the spectrometer.

Light Scattering. The 86.6-kg/mol POE and perdeuterated 59.2-kg/mol POE were analyzed at 25 °C using a Wyatt DAWN EOS multi-angle light scattering detector in chromatography mode (1 mL/min). Light scattered from a 30-mW solid-state laser (690 nm) was measured simultaneously at 17 angles. Sample concentrations were approximately 2 mg/mL, and injection volumes were 100 μL. Debye plots were constructed at half-second increments through the chromatogram. Root-mean-square radii (R_g) were determined from the slopes, and molar masses were determined from the y intercepts of these Debye plots. A previously determined specific refractive index (dn/dc) of 0.135 mL/g was used for both the hydrogenated and perdeuterated POE. Quasi-elastic measurements were also conducted with an on-line Wyatt QELS instrument (sampling rate = 125 ms). Light scattered into a single angle was used to determine hydrodynamic radii (R_h).

X-Ray Scattering. WAXD data for all samples were measured using either a Scintag, Inc. (USA) X1 Advanced Diffraction System with source run at 40 mA and 45 kV or a Philips PW1729 diffractometer run at 50 mA and 35 kV. Both instruments employed Cu K_α sources ($\lambda = 0.154$ nm) and were operated in a $\theta-2\theta$ scanning mode. A number of spectra were collected at the Daresbury Laboratory synchrotron radiation source (Cheshire, UK) using the two-circle diffractometer (station 2.3) operating with a λ of 0.14 nm.[22] Small-angle X-ray scattering (SAXS) patterns were recorded on a Rigaku MicroMax 002 Microfocus using an R-Axis IV++ detector. The copper anode was operated at 45 kV and 0.66 mA. The sample-to-detector path length was 802.5 mm (helium purged). All X-ray scattering data (SAXS and WAXD) were collected on dried powders.

Small-Angle Neutron Scattering. For the SANS measurements, the samples were prepared by pressing (2 tons of pressure) the powders into disks with 16-mm diameters and thicknesses between 0.66 and 1.91 mm. These samples were held in brass cells sandwiched between two quartz windows that were each 1.37-mm thick. In all these measurements, the cyclodextrins were fully hydrogenated but complexed with either 100% perdeuterated POE backbones or blends of 70% hydrogenated and 30% perdeuterated chains.

The SANS spectra were collected on the LOQ instrument at the ISIS Facility, Rutherford Appleton Laboratory, UK.[23] The instrument was operated in its conventional 25-Hz configuration, giving an effective momentum transfer range of $0.006 \leq \boldsymbol{q} \leq 0.24$ Å^{-1}, and the incident beam was apertured to a diameter of 10 mm. SANS data were collected at various temperatures from room temperature to 423 K using the LOQ thermostatically controlled sample changer. The scattering from these samples was found to be totally isotropic; in order to improve statistics, the data were radially averaged over the entire detector area. The raw scattering data were converted to absolute intensities using the standard reduction procedures. Using the FISH2 analysis package, the corrected SANS data were fitted to a two-phase paracrystalline model, which assumes randomly oriented lamellar stacks with a one-dimensional paracrystalline distortion. The fitting routine is based on the equations developed by a number of authors.[24−26] In essence, within the paracrystalline model, the scattering intensity can be described in terms of the form factor, $P(\boldsymbol{q})$, deriving from an infinite sheet, and the structure factor, $S(\boldsymbol{q})$, from a stack of such sheets. The description of the sheet allows for some waviness, which is included through a Lorentz-type factor.

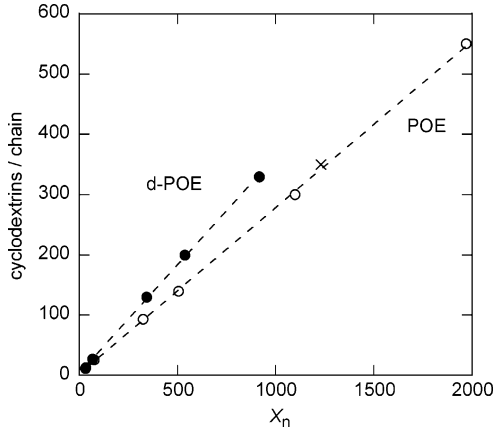

Figure 1. Cyclodextrins per chain versus number-average degree of polymerization for monodisperse POE (○) or perdeuterated POE (●) in their inclusion complexes with α-cyclodextrin. The × signifies the 59.2-kg/mol d-POE ($X_n = 1230$). Dashed lines are linear least-squares fits to the data.

Results and Discussion

Formation of Inclusion Complexes. Solid inclusion complexes were prepared from α-CD and monodisperse POE with molecular weights from 1.5 to 86.6 kg/mol. The characteristics of these complexes are shown in Table 1. Inclusion complexes were also prepared from α-CD and perdeuterated monodisperse POE with molecular weights from 1.5 to 59.2 kg/mol. The characteristics of these perdeuterated-POE complexes are shown in Table 2. With the exception of the two highest-molecular-weight perdeuterated POEs, the gravimetric yields for these complexes are 54−70% and exhibit no apparent trend with POE molecular weight. The yields drop off significantly for perdeuterated POE of 44 kg/mol (36% yield) and higher. While the inclusion-complex yield using 86.6-kg/mol POE is 64%, it is only 6.3% for the 59.2-kg/mol perdeuterated POE. Perdeuterated POE with higher molecular weights will not precipitate from aqueous solution as inclusion complexes with α-CD.

For all POEs, the number of cyclodextrins per chain increases with increasing molecular weight. However, as shown in Figure 1, the number of cyclodextrins per chain increases at a greater rate with chain length when the chain is perdeuterated. For both the hydrogenated and perdeuterated backbones, the relationship is linear: CD/chain = kX_n, where $k_{POE} = 0.28$ and $k_{d\text{-POE}} = 0.36$. The 59.2-kg/mol d-POE does not fit this trend (shown in Figure 1 as an ×), but this sample is probably not truly representative since it never resulted in sufficient solution turbidity to measure a threading time and was collected in only 6.3% yield (see Table 2). For the shortest chain lengths (1.5 kg/mol), there is no significant difference between hydrogenated and perdeuterated POE in the number of cyclodextrins per chain. However, for a given chain length greater than 1.5 kg/mol, perdeuterated POE backbones precipitate as inclusion complexes with a larger number of α-CDs.

The data of Figure 1 are consistent with molecular dynamics simulations reported by Pozuelo et al.[27] for POE/α-CD rotaxanes in which they concluded the "polymer captures as much α-CD as its length permits." This assertion was based on calculations that revealed binding energy, defined as the total potential energy of the complex after subtracting the potential energies of

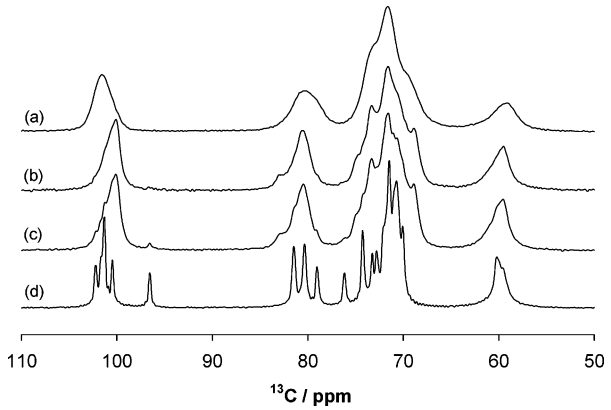

Figure 2. ^{13}C CP/MAS NMR spectra of (a) poly[(oxyethylene)-*rotaxa*-(α-cyclodextrin)],[8] (b) the α-CD/POE inclusion complex formed from equimolar quantities of α-CD and POE with X_n = 77 (3.4 kg/mol), (c) the same α-CD/POE inclusion complex formed with a 10% excess of α-CD, and (d) α-CD hexahydrate. The inclusion complexes described here (b and c) were prepared by simply mixing aqueous solutions of α-CD and POE followed by drying without filtration and without washing the solid product (thus, the yields are 100%).

the isolated CDs and POE, decreases as a function of the number of cyclodextrins on a chain. This was attributed to the cumulative stabilization of the complex by the interaction of threaded CDs with their neighbors. They examined only short POE chains (8 or 10 oxyethylene units) and did not consider such potential impediments to complete threading as gelation.

The number of cyclodextrins per chain is determined by NMR spectroscopy of the solid inclusion complex dissolved in DMSO-d_6. Once dissolved in DMSO, none of the cyclodextrins are threaded on the chain,[8] so the data of Figure 1 do not distinguish between threaded and unthreaded cyclodextrins in the solid inclusion complexes. In fact, Harada and Kamachi[4] showed that both threaded and unthreaded cyclodextrins were contained within freeze-dried gels prepared from PEGs with molecular weights of 2−900 kg/mol; using wide-angle X-ray diffraction, they reported that the relative fraction of unthreaded cyclodextrins increased with increasing PEG molecular weight. Those gels were formed with a stoichiometric 2:1 ratio of PEG repeat units to cyclodextrins, and no indication was given that the gels were washed to remove unthreaded components prior to freeze-drying. While our gels were formed in the presence of a near stoichiometric ratio (PRU:CD = 2.3), they were washed and then isolated with less than the total weight of the starting materials. The yields in Tables 1 and 2 primarily result from loss of cyclodextrins during the washing procedure, which represent over 90% of the weight of the starting materials.

Solid-state NMR data are typically provided as evidence for threaded cyclodextrins and a channel-like structure in these solid inclusion complexes.[2] Figure 2 shows the ^{13}C CP/MAS NMR spectra of α-CD, α-CD/POE_{77} inclusion complexes, and an α-CD/POE_{77} inclusion complex for which the POE_{77} ends have been blocked to yield a true polyrotaxane, poly[(oxyethylene)-*rotaxa*-(α-cyclodextrin)].[8] The polyrotaxane was thoroughly washed and characterized by DOSY NMR to confirm without ambiguity that the cyclodextrins in this material are threaded (average per chain = 14).[8] The inclusion complexes (Figure 2b and c) were prepared by simply mixing aqueous solutions of α-CD and POE_{77} followed by drying without filtration and without washing the solid product; thus, none of the cyclodextrins were removed from these samples (the gravimetric yields were 100%). Figure 2b is the ^{13}C CP/MAS NMR spectrum of an inclusion complex prepared with stoichiometric quantities of α-CD and POE_{77}, based on a PRU:CD ratio of 2:1, to give an average of 39 cyclodextrins per chain. Figure 2c is the ^{13}C CP/MAS NMR spectrum of an inclusion complex prepared with 10% excess α-CD to give an average of 42 cyclodextrins per chain.

Compared to the NMR spectrum of the crystalline α-CD (Figure 2d), the NMR spectra of the rotaxanated polymers contain broader peaks. This is due to the lower overall crystallinity of these materials as compared to the α-CD.[28] Actually, the NMR spectrum shown in Figure 2d also represents an inclusion complex, the hexahydrate form of α-CD.[29] It contains two water molecules inside the CD cavity (and four outside).[30] The NMR peak positions and multiplicities have been correlated with associated torsional angles for three of the carbons within the α-CD framework.[29,31] The peaks from 96 to 103 ppm are due to the anomeric carbon (typically designated carbon 1), located between the two in-chain oxygens. In the hexahydrate, the six anomeric carbons of α-CD reside in five distinct environments defined by the torsional-angle relationships of their respective neighboring atoms. This is manifested by the appearance of five different peaks in the solid-state NMR spectrum: 96.6, 100.5, 101.3, 101.7 (shoulder in Figure 2d), and 102.2 ppm. The peak at 101.3 ppm is twice the intensity of the other peaks, thus accounting for the sixth carbon. In other words, two of the six carbons exist in similar environments. While four of the anomeric carbon peaks appear clustered near 100 to 102 ppm, one is shifted upfield by 4 ppm to 96.6 ppm. In the crystal structure of α-CD hexahydrate, one of the six glucose rings is rotated nearly 90° with respect to the other five rings (and the CD channel) to facilitate hydrogen bonding to intracavity water.[30] Consequently, the anomeric carbon of this ring is nearly gauche to carbon 5 of the adjacent ring (torsional angle, $\phi = -69.3°$); all of the other anomeric carbons exhibit torsional angles from 103 to 124°. The additional shielding by a γ gauche carbon causes the upfield shift[32] that is observed as the peak at 96.6 ppm. This peak typically disappears when the intracavity water is replaced with larger guests since the glucose ring perpendicular to the CD channel orients along with the other glucose rings parallel to the CD channel. In some cases, the CD ring is more symmetrical and the chemical shifts of each carbon appear as sharp peaks. On the other hand, transformation of the highly crystalline α-CD hexahydrate to a less crystalline material may lead to the disappearance of the peak at 96.6 ppm, without the formation of a highly symmetrical CD ring. This is exactly what is observed for the rotaxanated polymers in Figure 2a−c, in which the peaks are not at all sharp, but broad, representing a distribution of conformations. Indeed, the peak widths at the baseline are nearly the same as that observed for the uncomplexed α-CD (Figure 2d). In fact, complete dehydration of α-CD results in a ^{13}C solid-state NMR spectrum consisting of broadened peaks for each carbon that encompass the same chemical-shift ranges as the respective discrete peaks observed for α-CD hexahydrate (Figure 2d).[33] In these cases, the broadened peaks simply represent a distribution of associated torsional angles for each of the carbons within the CD ring. The

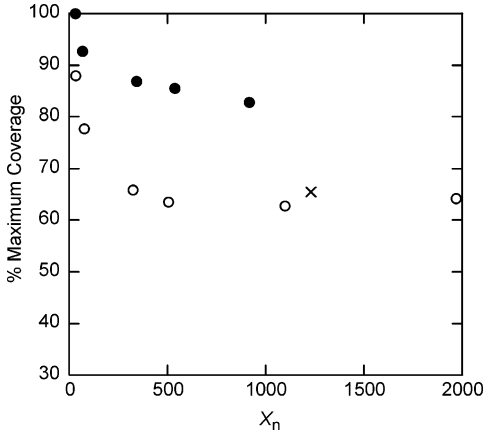

Figure 3. Maximum coverage (%) versus number-average degree of polymerization for monodisperse POE (○) or perdeuterated POE (●) in their inclusion complexes with α-cyclodextrin. The × signifies the 59.2-kg/mol *d*-POE ($X_n = 1230$).

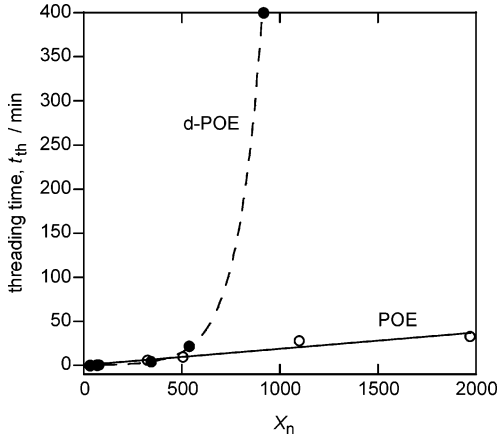

Figure 4. Threading time (i.e., time until gelation) versus number-average degree of polymerization for monodisperse POE (○) and perdeuterated POE (●) in their inclusion complexes with α-cyclodextrin. The solid line is a linear least-squares fit to the POE data, and the dashed line is an exponential fit to the *d*-POE data.

peak maximum for the polyrotaxane (101.4 ppm, Figure 2a) is downfield from the maxima for the polypseudorotaxanes (100 ppm, Figure 2b and c), indicating the cyclodextrins in these polypseudorotaxanes adopt conformations that generally shield the anomeric carbons to a greater extent.

The appearance of the 96.6-ppm peak in the spectrum for the inclusion complex formed with a 10% excess of α-CD (Figure 2c) indicates the presence of some α-CD hexahydrate in this sample. If the spectral intensities were quantitative, this peak should be about 1.6% (one-sixth of 10%) of the total anomeric carbon intensity, which is consistent with that observed. For the inclusion complex prepared with stoichiometric quantities of α-CD and POE_{77} (Figure 2b), there is no peak at 96.6 ppm and therefore no α-CD hexahydrate in the sample; the conclusion here is that all of the cyclodextrins are threaded. For all of the CD/POE inclusion complexes prepared for this study and described in Tables 1 and 2, there is no peak at 96.6 ppm in their respective ^{13}C CP/MAS NMR spectra.

Assuming all of the cyclodextrins are threaded, the percentage coverage of the backbones can be calculated. This is shown in Tables 1 and 2 and plotted in Figure 3 as the percentage maximum coverage versus number-average degree of polymerization. While these POE backbones can include one α-CD per two repeat units (PRU), the maximum coverage is limited here by the PRU:CD ratio in the originating solutions. For the low-molecular-weight backbones, full or nearly full coverage is achieved. For higher molecular weights, threading is interrupted and consequently limited by gel formation. The percentage coverage decreases with increasing molecular weight and becomes relatively constant for $X_n = 500$ and above: about 65% for the hydrogenated backbones and 85% for the perdeuterated backbones. For a given X_n, the perdeuterated POE is more highly threaded than the hydrogenated POE.

The number of cyclodextrins per chain should be related to the length of time the complex remains in solution. The threading time is shown in Figure 4 as a function of the number-average degree of polymerization for the hydrogenated and perdeuterated POE. For both backbones, the threading time increases with increasing molecular weight. This is due to the decreased concentration of end groups and the presence of longer unthreaded segments with increasing molecular weight; the end groups are the sites for initial complexation and the unthreaded segments maintain solvation. For X_n less than about 500, there is no experimentally significant difference in the threading times. However, above $X_n = 500$, the trend in the threading times diverges for the perdeuterated backbones, which thread more slowly, and the hydrogenated backbones, which thread more rapidly. The threading time for the hydrogenated backbones is linear with molecular weight; this has been reported previously[4] and is shown in Figure 4 as the solid linear line: $t_{th} \approx 0.018X_n$. The threading time for the perdeuterated backbones is exponential with molecular weight up to 44 kg/mol ($X_n = 917$): $t_{th} = 0.28 \exp(0.008X_n)$.

Using a transition-state model, Ceccato et al. derived an expression relating the threading time with the number of cyclodextrins per chain (m) and the Gibbs free energy of formation ($\Delta G^{\ddagger}$) of an activated complex.[10] In that work, the threading time was measured as a function of temperature and the number of cyclodextrins per chain was calculated along with the Gibbs free energy of activation. For a chain length of 76 repeat units ($M_n = 3.35$ kg/mol), they predicted an m value of 20 ± 2. For $M_n = 3.4$ kg/mol POE, we measured 26 cyclodextrins per chain.

The times required for gel formation, t_{th}, were longer for perdeuterated POE with X_n above ~500, indicating slower product formation rates for perdeuterated chains. When the perdeuterated POE backbone reached 60 kg/mol, complexes would not form. This isotope effect is pronounced. Possible explanations must be based on differences between the perdeuterated POE chain and the hydrogenated POE chain in water. For example, the perdeuterated POE may exhibit a decreased driving force for inclusion into CD, decreased availability of its chain ends, or both. The decreased driving force for CD inclusion could be due to the shorter $C-^2H$ bond length compared to $C-^1H$ bonds, which leads to lower polarizabilities and smaller segment volumes[34,35] for perdeuterated POE. The decreased availability of the perdeuterated POE chain ends could be due to the stronger tendency of perdeuterated POE to form clusters in solution as compared to hydrogenated POE,[36] as well as a more collapsed chain structure as the second virial coefficient decreases with increasing POE molecular weight.[37,38]

Table 3. Monodisperse POE and *d*-POE in Dilute Aqueous Solution (0.1%)

	M_w (kg/mol)[a]	M_n (kg/mol)	rms radius, R_g (nm)	hydrodynamic radius, R_h (nm)	$R_g/\sqrt{X_w}$ (nm)	R_g/R_h
POE	82 ± 1	82 ± 1	15 ± 1	9.5 ± 0.5	0.35	1.58
d-POE	61 ± 1	61 ± 1	13 ± 1	8.5 ± 0.5	0.36	1.53

[a] Previously determined dn/dc = 0.135 used for both POE and *d*-POE.

Cluster formation has been repeatedly observed for dilute aqueous POE solutions by static and dynamic light scattering, gel permeation chromatography,[39] viscometry, and SANS.[36,40] The clusters form above a critical concentration by aggregation of individual polymer coils. Vigorous stirring does not break up the clusters. They can be removed by filtration, do not form in chloroform solutions, and break up with increasing temperature. After clusters are removed from aqueous solutions, they will reform to reach an equilibrium amount. For monodisperse hydrogenated POE with M_w of 100 kg/mol, the critical concentration for cluster formation in D_2O is 0.4% at 10 °C.[36] This concentration should be higher at higher temperatures, for lower-molecular-weight POE, and in H_2O. Our POE/CD complexes were prepared by mixing 4.8% POE aqueous solutions into saturated CD solutions, giving a final POE concentration of 1.2%.

In a very nice demonstration of the isotope effect in cluster formation in POE/water solutions, the viscosity was measured for 4% POE (100 kg/mol) solutions and the following trend was observed: *d*-POE in D_2O > POE in D_2O > *d*-POE in H_2O > POE in H_2O.[36] The highest viscosity was exhibited by the solution (*d*-POE in D_2O) with the strongest tendency to form clusters as observed by SANS. In water, perdeuterated POE forms clusters more readily than hydrogenated POE.

Adding a drop of chloroform to filtered POE solutions prevents re-formation of the clusters.[41] We prepared inclusion complexes of POE_{507} and *d*-POE_{538} by the standard procedure but modified it by adding a drop of chloroform to the POE solutions followed by 10 min of ultrasonication. Following ultrasonication, another drop of chloroform was added to each solution before the saturated α-CD solution was added. The solution mixture was ultrasonicated for another 10 min, and the solutions were monitored for gelation. Following the 10-min sonication, the hydrogenated POE solution was already opaque due to gelation, while the perdeuterated POE solution was barely translucent. Twenty five minutes after the POE solutions were mixed with the α-CD solutions, the hydrogenated POE was completely gelled, while the perdeuterated POE solution could still be poured out of the vial. Thus, the threading times appeared to be very similar to the threading times reported in Tables 1 and 2 (10 and 22 min for POE and *d*-POE, respectively). Chloroform addition and sonication of the POE solutions did not have an effect.

We examined the two highest-molecular-weight POE samples with static and dynamic light scattering to determine whether any obvious conformational differences could be related to the very different gelation kinetics that were observed. The solution concentrations were 0.1% (w/v), which is lower than that expected for cluster formation, and the samples were measured in chromatography mode. The results are shown in Table 3. The root-mean-square radius of gyration (R_g) of the 86.6-kg/mol hydrogenated POE in water is 15 ± 1 nm, while the R_g of the 59.2-kg/mol perdeuterated POE is 13 ± 1 nm. To compare these two POEs, the R_g values were normalized by the square root of the chain length. The $R_g/\sqrt{X_w}$ values are nearly indistinguishable, revealing that perdeuteration does not significantly affect the size of these isolated polymers in dilute aqueous solution. The ratios of R_g's to hydrodynamic radii are also nearly equivalent for both polymers (1.5−1.6), and denote random coils in good solvents. Hydrogen bonding of water to the POE chain is not expected to be significantly different for the hydrogenated and perdeuterated POE. Thus, during complexation, solvation of partially threaded chains should remain relatively unaffected for the *d*-POE compared to the POE and therefore not influence the observed differences in gelation kinetics.

In summary, the perdeuterated POE chains larger than $X_n = 500$ exhibit slower gelation than the hydrogenated POE of similar chain length, while the gelation times are comparable for shorter chain lengths. The differences in the formation kinetics are attributed to either weaker driving forces for α-CD inclusion, a stronger tendency to cluster for perdeuterated POE, or both. The difference in the driving forces for threading are not significant for the low-molecular-weight backbones but become obvious as the overall threading rate is decreased due to the lower concentration of chain ends in the higher-molecular-weight backbones. Furthermore, clustering is expected to be much more significant with the high-molecular-weight backbones and for the perdeuterated POE. The threading rate is reduced, subsequently delaying the formation of hydrogen-bonded CD stacks along the chain required for gelation. The perdeuterated chains remain in solution longer and become more highly threaded before gelation occurs. The structural consequences for this isotope-induced kinetic effect are described below.

Characterization of Solid Inclusion Complexes. Representative WAXD patterns of the inclusion complexes formed from POE and perdeuterated POE are shown in Figure 5 for three different backbone molecular weights. The position of the major diffraction peaks are the same as those reported for cyclodextrin inclusion complexes crystallized in the channel structure[3,42] and markedly different from the native POE and α-CD diffraction patterns. By slowly recrystallizing α-CD/POE complexes, Hwang et al.[42] prepared microfibers and indexed their X-ray diffraction patterns to a hexagonal unit cell. They used low-molecular-weight POE (2 kg/mol) to prepare their inclusion complexes, and their WAXD patterns, prior to recrystallization, match those shown in Figure 5 for our complexes prepared from POE_{77} and *d*-POE_{67}. For both POE and perdeuterated POE, as the molecular weight of the polymer backbone increases, there is an overall decrease in crystallinity. This is consistent with the increasing tendency toward gel formation with increasing molecular weights.

For the complexes prepared from the two lower-molecular-weight POEs (POE, $X_n = 77$ and 325; *d*-POE, $X_n = 67$ and 344), the WAXD peaks for the perdeuterated POE complexes are slightly sharper (i.e., smaller half-widths) than those for the analogous hydrogenated

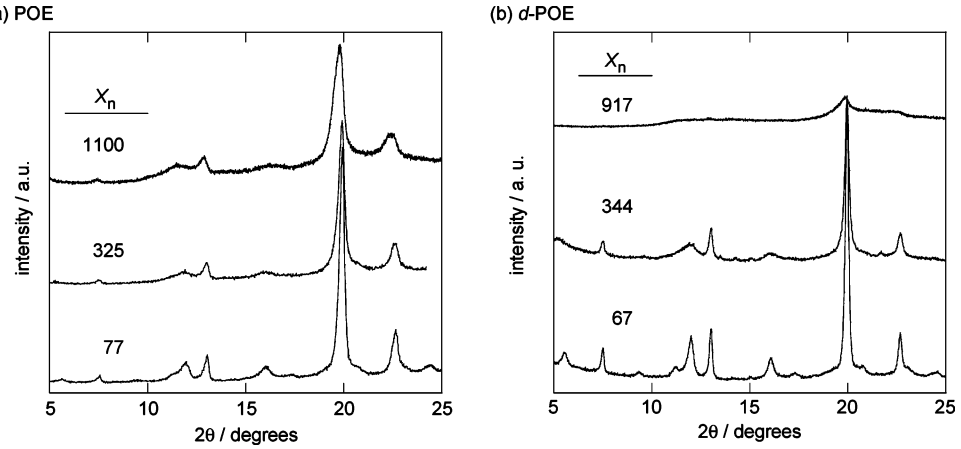

Figure 5. Wide-angle X-ray diffractograms of α-CD inclusion complexes with (a) poly(oxyethylene) with molecular weights of 48.5 (X_n = 1100), 14.3 (X_n = 325), and 3.4 kg/mol (X_n = 77); and with (b) perdeuterated poly(oxyethylene) with molecular weights of 44 (X_n = 917), 16.5 (X_n = 344), and 3.2 kg/mol (X_n = 67).

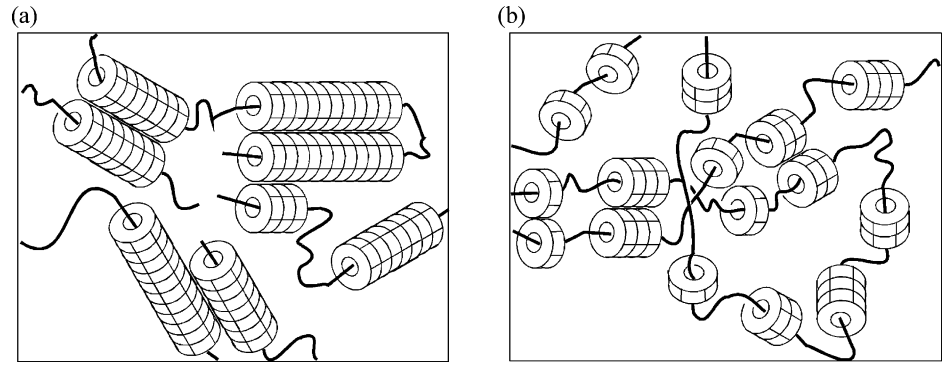

Figure 6. Schematic morphology proposed for the POE/α-CD inclusion complexes for (a) hydrogenated POE and perdeuterated POE with X_n < 500, and (b) perdeuterated POE with X_n > 500. The longer α-CD stack lengths are manifested as higher crystallinity (see Figure 5). The longer stacks are a result of sufficiently fast threading kinetics (see Figure 4) that facilitate formation of inter-CD hydrogen bonding before diffusion along the chain separates individual cyclodextrins and gives the more amorphous structure observed when X_n = 917 perdeuterated POE is used.

POE complexes. Even so, these complexes have the same crystal structure and approximately the same degree of crystallinity and crystallite size. On the other hand, the complex prepared from the high-molecular-weight *d*-POE (X_n = 917) contains very little crystallinity, in stark contrast to the analogous hydrogenated POE_{1100} or the complexes formed from the lower-molecular-weight POEs.

These diffraction data indicate that the complexes prepared from the two lower-molecular-weight perdeuterated POEs are composed of slightly larger crystallites than the complexes of similar-length hydrogenated POEs. This is consistent with the results displayed in Figures 1 and 3, where higher degrees of threading were observed for a given POE chain length when the POE is perdeuterated. This same explanation is obviously not valid for the higher-molecular-weight backbones, where the crystallinity is seemingly not correlated to the higher threading ratio on the perdeuterated chains. The difference for these higher-molecular-weight chains is the very different kinetics of formation. The threading times are similar for both backbones until X_n = 500 is reached (cf. Figure 4), at which chain length the threading times are significantly longer and the yields lower for the perdeuterated chains. With longer threading times, a newly threaded cyclodextrin has more time to diffuse along the chain before the subsequent cyclodextrin is threaded. Thus, threaded cyclodextrins can become more separated along the chain so that formation of the hydrogen-bonded stacks, required for gelation, is delayed. The resulting morphology of this model is schematically depicted in Figure 6.

SANS and SAXS studies were used to further examine the morphology of the solid POE/α-CD inclusion complexes. Representative SANS data for the complexes prepared from 100% *d*-POE are shown in Figure 7 as a function of *d*-POE molecular weight. For the $d\text{-}POE_{344}$, $d\text{-}POE_{538}$, and $d\text{-}POE_{917}$ complexes, there is a maximum observed at $\boldsymbol{q}$ values between 0.07 and 0.10 $Å^{-1}$. The maximum for the $d\text{-}POE_{917}$ complex is rather broad and diffuse compared to that of the $d\text{-}POE_{344}$ and $d\text{-}POE_{538}$ complexes. The scattering from the $d\text{-}POE_{31}$ and $d\text{-}POE_{67}$ complexes (only one is shown in Figure 7) decreases monotonically without any evidence of the maximum observed for the higher-molecular-weight analogues. These two lower-molecular-weight *d*-POEs are nearly completely covered with cyclodextrins, while the three higher-molecular-weight POEs are not (see Figure 3). Thus, the three higher-molecular-weight POEs contain higher fractions of unthreaded deuterated chain segments, which exhibit a higher scattering-length density than the cyclodextrin-threaded segments (i.e., α-CD stacks). The maxima in Figure 7 are attributed to discrete scattering by regularly spaced unthreaded *d*-POE segments between the α-CD stacks. This peak for the highest-molecular-weight *d*-POE complex (X_n = 917) is less pronounced because the cyclodextrin stacks are less defined for this sample (see Figures 5b and 6b). The SAXS data for all the various molecular weight samples show similar scattering be-

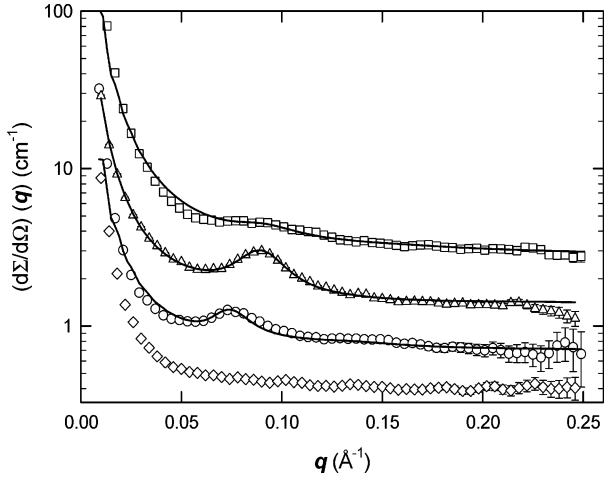

Figure 7. Small-angle neutron scattering data for α-CD inclusion complexes with 100% *d*-POE with molecular weights of 1.5 ($X_n = 31$) (◇), 16.5 ($X_n = 344$) (○), 25.8 ($X_n = 538$) (△), and 44 kg/mol ($X_n = 917$) (□). The solid lines represent the best fits to the data using a two-phase paracrystalline model. All but the α-CD/*d*-POE$_{344}$ curve (○) have been translated along the *y* axis for clarity.

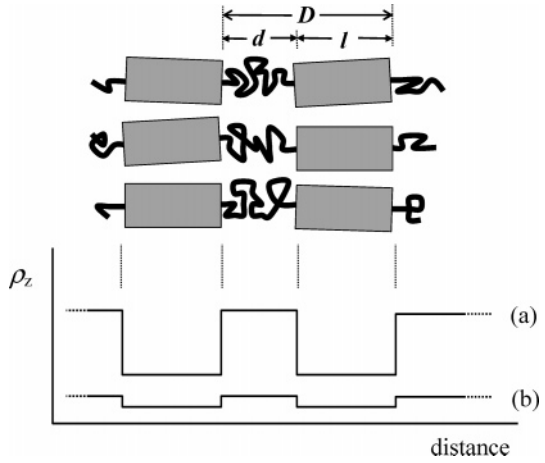

Figure 8. Schematic showing alternating layers of amorphous and crystalline domains which are made up from unthreaded *d*-POE chains (heavy black lines) and crystalline α-CD/*d*-POE stacks (grey rectangular boxes). Shown on the lower part of the plot are the corresponding neutron-scattering-length density (ρ_z) profiles for samples prepared from (a) 100% and (b) 30% perdeuterated POE.

havior with a decrease in intensity with increasing $\boldsymbol{q}$ vector. Unfortunately, unlike the SANS data, the features which are present within the scattering curves are insufficiently defined to fit the data unambiguously. Further work on SAXS analysis of these samples is in progress.

The SANS scattering behavior is similar to that observed for semicrystalline polymers in which a deuterated solvent is absorbed into the interlamellar amorphous regions.[43] Such data may be fit with a two-phase distorted multilayer-stack paracrystalline model.[24−26] The model consists of randomly oriented stacks of alternating layers of crystalline lamellae and amorphous domains. Although by definition of the paracrystalline model these layers are considered to be of infinite extent, this is with respect to the wavelength of the neutrons of the probe used, which for LOQ is 1.0 nm or less. The scattering from these paracrystalline materials can therefore be separated into two components.[43−46] The observed maxima arise from discrete scattering produced by periodic fluctuations in scattering-length density created by alternating crystalline (i.e., α-CD/*d*-POE stacks) and amorphous (i.e., unthreaded *d*-POE) layers. Diffuse scattering from the amorphous material outside the lamellar regions contributes to the low-$\boldsymbol{q}$ intensity. Additional signal from the incoherent neutron scattering which contributes to the high-$\boldsymbol{q}$ background was also taken into account. In the lamellar regions, there is assumed to be a finite number of infinite planes of alternating amorphous and crystalline material, shown schematically in Figure 8. A schematic plot of the scattering-length density across the amorphous and crystalline lamellae is also shown for two cases where there is either a large (a) or a small (b) difference in contrast. This is the case for the samples prepared with 100% *d*-POE (large contrast) or 30% *d*-POE (small contrast). Thus, the model parameters correspond to the crystalline α-CD stack thickness, *l*, the unthreaded-POE amorphous layer thickness, *d,* and the characteristic repeat spacing, $D = d + l$. Within the model framework, a distortion factor was used which effectively allows for imperfections in the crystalline α-CD stacks.

With the exception of the two lower-molecular-weight POE complexes (X_n = 31 and 67), the scattering behavior was analyzed assuming this two-phase paracrystalline model. The parameters used in fitting the scattering curves are given in Table 4, and the fits are shown as solid lines in Figure 7. Thickness parameters were confirmed by fitting the partially deuterated complexes (prepared by mixing perdeuterated with hydrogenated POE) while holding these values constant and only varying the scattering-length densities, that is, using a scattering-length density profile given by Figure 8b. A representative fit to the scattering curve for the α-CD/POE$_{538}$ complex (30% *d*-POE) is shown in Figure 9 to be in excellent agreement with the data. A very shallow maximum, just visible at $\boldsymbol{q} \approx 0.09$ Å^{-1}, is the remnant of the peak observed for the α-CD/POE$_{538}$ complex prepared from 100% *d*-POE. From these fits, we can say for certain that the lamellar regions with high neutron-scattering-length density must be associated with unthreaded POE, which cannot close pack to each other to crystallize, and therefore acts as an amorphous spacer. The crystalline lamellae are therefore regions of POE threaded by α-CD.

There is a noticeable shift in the position of the SANS maxima in Figure 7 to higher $\boldsymbol{q}$ values, indicating a reduction in the repeat length of the crystalline CD stacks ($D = 2\pi/\boldsymbol{q}$), as the *d*-POE chain length increases. The $\boldsymbol{q}$-value shift from approximately 0.075 to 0.09 Å^{-1} corresponds to a decrease in the stack repeat length from 8.4 to 6.5 nm (see Table 4). The broadening in the maxima which accompanies this change in *D* is attributed to a significant degree of crystalline distortion. In this model, this is represented by an increase in the error in the dimensions of the phases, particularly in the value of *l*. This dimension, the α-CD/*d*-POE stack length, can be used to estimate the average number of α-CDs per crystalline stack: $n = l/0.806$, where 0.806 is the depth of a single α-CD cavity.[27] The POEs represented in Table 4 are partially covered, which alone does not explain the aggregation of threaded cyclodextrins into small hydrogen-bonded stacks. The unthreaded chain sections, through conformational dynamics, may provide an effective barrier to close approach of adjacent CDs and thereby prevent stack formation. The stack length decreases with increasing *d*-POE chain length. Thus, while the longer chains have

Table 4. Fit Parameters for Two-Phase Paracrystalline Model Applied to SANS Data for Perdeuterated POE/α-CD Inclusion Complexes at 297 K

	dimensions (nm)			
complex	unthreaded *d*-POE layer, *d*	α-CD/*d*-POE stack, *l*	stack repeat length, *D*	α-CD per stack,[a] *n*
α-CD/*d*-POE_{344}	2.70 ± 0.13	5.66 ± 0.38	8.36 ± 0.25	7.02 ± 0.47
α-CD/*d*-POE_{538}	3.48 ± 0.09	3.26 ± 0.11	6.74 ± 0.02	4.04 ± 0.14
α-CD/*d*-POE_{917}	5.05 ± 0.30	1.45 ± 0.69	6.5 ± 0.39	1.80 ± 0.85

[a] Calculated by assuming an α-CD depth of 0.806 nm.[27]

Table 5. Fit Parameters for Two-Phase Paracrystalline Model Applied to SANS Data for α-CD Inclusion Complexes with 25.8-kg/mol Perdeuterated POE (X_n = 538)

		dimensions (nm)			
PRU:CD	*T* (K)	unthreaded *d*-POE layer, *d*	α-CD/*d*-POE stack, *l*	stack repeat length, *D*	α-CD per stack,[a] *n*
2.7	297	3.48 ± 0.09	3.26 ± 0.11	6.74 ± 0.02	4.04 ± 0.14
	373	4.00 ± 0.17	2.66 ± 0.23	6.66 ± 0.06	3.30 ± 0.28
	423	4.11 ± 0.04	2.56 ± 0.06	6.67 ± 0.02	3.17 ± 0.07
5	297	2.53 ± 0.24	4.34 ± 0.34	6.87 ± 0.10	5.38 ± 0.42
	373	4.94 ± 0.01	1.45 ± 0.02	6.39 ± 0.01	1.80 ± 0.03
	423	4.81 ± 0.05	1.49 ± 0.09	6.30 ± 0.04	1.85 ± 0.11

[a] Calculated by assuming an α-CD depth of 0.806 nm.[27]

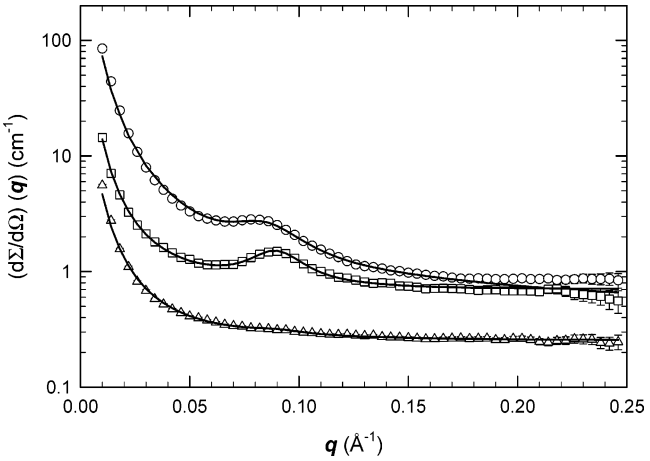

Figure 9. Small-angle neutron scattering data for α-CD inclusion complexes with 25.8-kg/mol *d*-POE (X_n = 538): 100% *d*-POE_{538} (□), 30% *d*-POE_{538} (△), and 100% *d*-POE_{538} at a reduced threading level (PRU:CD = 5)[47] (○). Some data (□ and △) are scaled by 0.25 for clarity. The solid lines represent best fits assuming a two-phase paracrystalline model.

shorter α-CD stacks and therefore fewer cyclodextrins per stack, they do require a greater total number of cyclodextrins to thread before gelation occurs (cf. Figure 1).

For a given POE chain length (>∼1.5 kg/mol), the threading level may be controlled by varying the POE concentration in the originating solution. Increasing the POE concentration in the originating solution causes faster gelation, yielding complexes with lower threading levels. Using the 25.8-kg/mol *d*-POE, an α-CD complex was prepared from an originating solution containing twice the concentration of *d*-POE (300 mg/11 mL water).[47] The SANS curve for this sample (reduced-threading-level α-CD/*d*-POE_{538}) is shown in Figure 9 along with the SANS curve for the 25.8-kg/mol *d*-POE complex described in Table 2. Both curves were fit assuming the two-phase paracrystalline model using the fit parameters listed in Table 5 and the scattering-length density profile shown in Figure 8a. While the stack repeat length is roughly equivalent for these two samples, there is a slight increase in the CD stack length and a consequent decrease in the unthreaded *d*-POE layer for the α-CD/*d*-POE_{538} complex with reduced threading level. The peak ($q \approx 0.085$ Å^{-1}) for this sample is, however, broader, suggesting a slightly more disordered crystalline structure, than the peak observed for the more highly threaded α-CD/*d*-POE_{538} complex ($q \approx 0.09$ Å^{-1}). In fitting the data, an 8−10% degree of distortion was allowed in the thickness values. Without this factor, the peak would have a much narrower width.

At elevated temperatures (373 and 423 K), both α-CD/*d*-POE_{538} complexes demonstrate similar scattering behavior to that seen at room temperature. Fitting the paracrystalline model as for the room-temperature samples gives the parameters shown in Table 5. The value of the *D* spacing remains fairly constant for the α-CD/*d*-POE_{538} complex with PRU:CD = 2.7, but drops for the α-CD/*d*-POE_{538} complex with reduced threading level so that its *D* spacing is now less than that for the α-CD/*d*-POE_{538} complex with PRU:CD = 2.7. In both inclusion complexes, the α-CD stack size (*l*) decreases; this is most notable for the reduced-threading-level α-CD/*d*-POE_{538} complex, where *l* drops by approximately 66% from its room-temperature value, compared to a 22% reduction for the α-CD/*d*-POE_{538} complex with PRU:CD = 2.7. This reduction in *l* leads to a corresponding drop in the average number of α-CD rings per stack. These changes may simply reflect the extra unthreaded-chain-segment space in the reduced-threading-level α-CD/*d*-POE_{538} complex. Upon heating, inter-CD hydrogen bonds can break and the conformational dynamics of the unthreaded chain segments may facilitate spreading of the CDs between the broken stacks and the previously unthreaded *d*-POE.

Summary

Perdeuterated poly(oxyethylene) (*d*-POE) backbones were rotaxanated with α-CD for SANS studies of the morphology. For molecular weights ≤3.2 kg/mol, the backbone is nearly completely covered with cyclodextrins. For molecular weights >3.2 kg/mol, the backbone is partially covered with cyclodextrins that aggregate to form crystalline hydrogen-bonded stacks that are separated by amorphous layers of unthreaded *d*-POE. As the *d*-POE molecular weight increases, the size of the crystalline α-CD stacks decreases. For molecular weights of 44 kg/mol, the stack size has decreased to the point that the materials exhibit very low crystallinity by WAXD, even though 83% of the chain is covered with cyclodextrins. This low crystallinity is

attributed to the very slow threading rate in solution (400 min to gelation) since a hydrogenated chain of similar molecular weight threads within 28 min and exhibits much higher crystallinity. The morphology differences between the low- and high-molecular-weight *d*-POE complexes with α-CD govern the POE chain dynamics, which has been documented using ^{2}H solid-state NMR spectroscopy.[48]

Acknowledgment. This work was supported by the National Science Foundation (DMR-0072876). Les Gelbaum of the Georgia Tech NMR Center suggested and assisted with the use of the relaxation agent for quantitative ^{13}C NMR. The SANS and WAXD studies were made possible by an International Collaborative Research Grant from the NATO Scientific Affairs Division. The light scattering data were collected by Michelle Chen of Wyatt Corporation (Santa Barbara, CA). R. K. Heenan of the ISIS Facility, Rutherford Appleton Laboratory (Chilton, Didcot, UK) kindly provided use of the FISH2 program. C. C. Tang of the Daresbury Laboratory (Cheshire, UK) collected some X-ray diffraction data on the synchrotron radiation source (SRS). The SAXS data were provided by Marilyn Minus and Satish Kumar of Georgia Tech. We gratefully acknowledge stipend support from the Georgia Tech Molecular Design Institute, under prime contract N00014-95-1-1116 from the Office of Naval Research.

References and Notes

(1) Harada, A.; Kamachi, M. *Macromolecules* **1990**, *23*, 2821−2823.
(2) Harada, A.; Li, J.; Kamachi, M. *Macromolecules* **1993**, *26*, 5698−5703.
(3) Harada, A. *Coord. Chem. Rev.* **1996**, *148*, 115−133.
(4) Li, J.; Harada, A.; Kamachi, M. *Polymer J.* **1994**, *26*, 1019−1026.
(5) Miyake, K.; Yasuda, S.; Harada, A.; Sumaoka, J.; Komiyama, M.; Shigekawa, H. *J. Am. Chem. Soc.* **2003**, *125*, 5080−5085.
(6) Huh, K. M.; Ooya, T.; Lee, W. K.; Sasaki, S.; Kwon, I. C.; Jeong, S. Y.; Yui, N. *Macromolecules* **2001**, *34*, 8657−8662.
(7) Li, J.; Ni, X.; Leong, K. W. *J. Biomed. Mater. Res.* **2003**, *65A*, 196−202.
(8) Zhao, T.; Beckham, H. W. *Macromolecules* **2003**, *36*, 9859−9865.
(9) Kawaguchi, Y.; Harada, A. *J. Am. Chem. Soc.* **2000**, *122*, 3797−3798.
(10) Ceccato, M.; Nostro, P. L.; Baglioni, P. *Langmuir* **1997**, *13*, 2436−2439.
(11) Harada, A.; Li, J.; Kamachi, M. *Nature* **1992**, *356*, 325−327.
(12) Lo Nostro, P.; Lopes, J. R.; Cardelli, C. *Langmuir* **2001**, *17*, 4610−4615.
(13) Lo Nostro, P.; Lopes, J. R.; Ninham, B. W.; Baglioni, P. *J. Phys. Chem. B* **2002**, *106*, 2166−2174.
(14) Huh, K. M.; Tomita, H.; Ooya, T.; Lee, W. K.; Sasaki, S.; Yui, N. *Macromolecules* **2002**, *35*, 3775−3777.
(15) Huang, L.; Allen, E.; Tonelli, A. E. *Polymer* **1999**, *40*, 3211−3221.
(16) Shuai, X.; Porbeni, F. E.; Wei, M.; Bullions, T.; Tonelli, A. E. *Macromolecules* **2002**, *35*, 2401−2405.
(17) Rusa, C. C.; Tonelli, A. E. *Macromolecules* **2000**, *33*, 5321−5324.
(18) Shuai, X.; Porbeni, F. E.; Wei, M.; Bullions, T.; Tonelli, A. E. *Macromolecules* **2002**, *35*, 3126−3132.
(19) Huang, L.; Allen, E.; Tonelli, A. E. *Polymer* **1998**, *39*, 4857−4865.
(20) Shuai, X.; Porbeni, F. E.; Wei, M.; Shin, I. D.; Tonelli, A. E. *Macromolecules* **2001**, *34*, 7355−7361.
(21) Porbeni, F. E.; Edeki, E. M.; Shin, I. D.; Tonelli, A. E. *Polymer* **2001**, *42*, 6907−6912.
(22) Roberts, M. A.; Tang, C. C. *J. Synchrotron Radiat.* **1998**, *5*, 1270−1274.
(23) http://www.isis.rl.ac.uk/largescale/loq/loq.htm.
(24) Wenig, W.; Braemer, R. *Colloid Polym. Sci.* **1978**, *256*, 125−132.
(25) Hall, I. H.; Mahmoud, E. A.; Carr, P. D.; Geng, Y. D. *Colloid Polym. Sci.* **1987**, *265*, 383−393.
(26) Kotlarchyk, M.; Ritzau, S. M. *J. Appl. Crystallogr.* **1991**, *24*, 753−758.
(27) Pozuelo, J.; Mendicuti, F.; Mattice, W. L. *Macromolecules* **1997**, *30*, 3685−3690.
(28) Gidley, M. J.; Bociek, S. M. *J. Am. Chem. Soc.* **1988**, *110*, 3820−3829.
(29) Veregin, R. P.; Fyfe, C. A.; Marchessault, R. H.; Taylor, M. G. *Carbohydr. Res.* **1987**, *160*, 41−56.
(30) Manor, P. C.; Saenger, W. *J. Am. Chem. Soc.* **1974**, *96*, 3630−3639.
(31) O'Brien, E. P.; Moyna, G. *Carbohydr. Res.* **2004**, *339*, 87−96.
(32) Tonelli, A. *NMR Spectroscopy and Polymer Microstructure*; VCH: New York, 1989.
(33) Heyes, S. J.; Clayden, N. J.; Dobson, C. M. *Carbohydr. Res.* **1992**, *233*, 1−14.
(34) Bates, F. S.; Fetters, L. J.; Wignall, G. D. *Macromolecules* **1988**, *21*, 1086−1094.
(35) Bates, F. S.; Keith, H. D.; McWhan, D. B. *Macromolecules* **1987**, *20*, 3065−3070.
(36) Hammouda, B.; Ho, D.; Kline, S. *Macromolecules* **2002**, *35*, 8578−8585.
(37) Kawaguchi, S.; Imai, G.; Suzuki, J.; Miyahara, A.; Kitano, T.; Ito, K. *Polymer* **1997**, *38*, 2885−2891.
(38) Dormidontova, E. E. *Macromolecules* **2004**, *37*, 7747−7761.
(39) Polverari, M.; van de Ven, T. G. M. *J. Phys. Chem.* **1996**, *100*, 13687−13695.
(40) Hammouda, B.; Ho, D. L.; Kline, S. *Macromolecules* **2004**, *37*, 6932−6937.
(41) Ho, D. L.; Hammouda, B.; Kline, S. R. *J. Polym. Sci., Part. B: Polym. Phys.* **2002**, *41*, 135−138.
(42) Hwang, M. J.; Bae, H. S.; Kim, S. J.; Jeong, B. *Macromolecules* **2004**, *37*, 8820−8822.
(43) Murthy, N. S.; Akkapeddi, M. K.; Orts, W. J. *Macromolecules* **1998**, *31*, 142−152.
(44) Murthy, N. S.; Stamm, M.; Sibilia, J. P.; Krimm, S. *Macromolecules* **1989**, *22*, 1261−1267.
(45) Cameron, R. E.; Donald, A. M. *Polymer 33*, 2628−2636.
(46) Jenkins, P. J.; Donald, A. M. *Polymer* **1996**, *37*, 5559−5568.
(47) The PRU:CD = 4.6 in the originating solution.
(48) Girardeau, T.; Leisen, J.; Beckham, H. W. *Macromol. Chem. Phys.* **2004**, provisionally accepted.

MA048756W